

# Loss-of-Function Variants in *MYLK* Cause Recessive Megacystis Microcolon Intestinal Hypoperistalsis Syndrome

Danny Halim,<sup>1</sup> Erwin Brosens,<sup>1</sup> Françoise Muller,<sup>2</sup> Michael F. Wangler,<sup>3,4,5</sup> Arthur L. Beaudet,<sup>3,4,5</sup> James R. Lupski,<sup>3,4,5,6,7</sup> Zeynep H. Coban Akdemir,<sup>3,6</sup> Michael Doukas,<sup>8</sup> Hans J. Stoop,<sup>8</sup> Bianca M. de Graaf,<sup>1</sup> Rutger W.W. Brouwer,<sup>9</sup> Wilfred F.J. van Ijcken,<sup>9</sup> Jean-François Oury,<sup>10</sup> Jonathan Rosenblatt,<sup>10</sup> Alan J. Burns,<sup>1,11</sup> Dick Tibboel,<sup>12</sup> Robert M.W. Hofstra,<sup>1,11,13,\*</sup> and Maria M. Alves<sup>1,13,\*</sup>

Megacystis microcolon intestinal hypoperistalsis syndrome (MMIHS) is a congenital disorder characterized by loss of smooth muscle contraction in the bladder and intestine. To date, three genes are known to be involved in MMIHS pathogenesis: *ACTG2*, *MYH11*, and *LMOD1*. However, for approximately 10% of affected individuals, the genetic cause of the disease is unknown, suggesting that other loci are most likely involved. Here, we report on three MMIHS-affected subjects from two consanguineous families with no variants in the known MMIHS-associated genes. By performing homozygosity mapping and whole-exome sequencing, we found homozygous variants in myosin light chain kinase (*MYLK*) in both families. We identified a 7 bp duplication (c.3838\_3844dupGAAAGCG [p.Glu1282\_Glyfs\*51]) in one family and a putative splice-site variant (c.3985+5C>A) in the other. Expression studies and splicing assays indicated that both variants affect normal *MYLK* expression. Because *MYLK* encodes an important kinase required for myosin activation and subsequent interaction with actin filaments, it is likely that in its absence, contraction of smooth muscle cells is impaired. The existence of a conditional-*Mylk*-knockout mouse model with severe gut dysmotility and abnormal function of the bladder supports the involvement of this gene in MMIHS pathogenesis. In aggregate, our findings implicate *MYLK* as a gene involved in the recessive form of MMIHS, confirming that this disease of the visceral organs is heterogeneous with a myopathic origin.

Contraction of smooth muscle cells (SMCs) results from an elaborate molecular process that involves the cross-bridge interaction between thin actin filaments and thick myosin filaments.<sup>1</sup> Loss of any of the proteins involved in this process is likely to affect cell physiology, resulting in impaired contractility. Recently, loss of SMC contraction has been found to underlie the development of megacystis microcolon intestinal hypoperistalsis syndrome (MMIHS [OMIM: 155310]), a rare congenital disease of the visceral organs, mainly characterized by bladder distension and the presence of a microcolon.<sup>2,3</sup> This link was made from the identification of pathogenic variants in three muscle-related genes: actin, gamma 2, smooth muscle, enteric (*ACTG2* [OMIM: 102545]),<sup>4–8</sup> myosin heavy chain 11 (*MYH11* [OMIM: 160745]),<sup>9</sup> and leimodin 1 (*LMOD1* [OMIM: 602715]).<sup>10</sup> De novo variants in *ACTG2* are implicated in the autosomal-dominant form of MMIHS,<sup>4–8</sup> whereas homozygous variants in *MYH11* and *LMOD1* cause a recessive form of the disease.<sup>9,10</sup> Although the identification of pathogenic variants in these genes explains approximately 90% of all MMIHS cases characterized by bladder and intestinal problems and for which genetic

information is available,<sup>4–10</sup> for some affected individuals, the causative mutation and associated gene have yet to be identified.

Here, we describe three MMIHS subjects from two independent families and for whom no variants in the known MMIHS-associated genes were found (Figure 1A). Subject 1 (II-2 in Figure 1A) was born to consanguineous parents of North African origin. Prenatal ultrasound performed at 13 weeks of gestation identified the presence of a distended bladder and a generalized subcutaneous edema (Figure 1B). Severe oligohydramnios was also reported. Autopsy of the fetus confirmed the diagnosis of MMIHS (the pregnancy was terminated at 15 weeks of gestation). Subject 2 (II-3 in Figure 1A) was the younger brother of subject 1. Distension of the bladder was observed on prenatal ultrasound (Figure 1C), and anhydramnios was detected. Labor occurred prematurely at 31 weeks of gestation. The neonate experienced respiratory distress and died. Further anamnesis revealed the presence of a distended bladder in the older sister (II-1 in Figure 1A) of subjects 1 and 2 before her intrauterine death at 30 weeks of gestation. Subject 3 (II-5 in Figure 1A) was the first child of a consanguineous

<sup>1</sup>Department of Clinical Genetics, Erasmus University Medical Center, 3000 CA Rotterdam, the Netherlands; <sup>2</sup>Biochimie Prenatale, Hôpital Universitaire Robert Debré, 75019 Paris, France; <sup>3</sup>Department of Molecular and Human Genetics, Baylor College of Medicine, Houston, TX 77030, USA; <sup>4</sup>Department of Pediatrics, Baylor College of Medicine, Houston, TX 77030, USA; <sup>5</sup>Texas Children's Hospital, Houston, TX 77030, USA; <sup>6</sup>Baylor-Hopkins Center for Mendelian Genomics, Baylor College of Medicine, Houston, TX 77030, USA; <sup>7</sup>Human Genome Sequencing Center, Baylor College of Medicine, Houston, TX 77030, USA; <sup>8</sup>Department of Pathology, Erasmus University Medical Center, 3000 CA Rotterdam, the Netherlands; <sup>9</sup>Erasmus Center for Biomics, Erasmus Medical Center, 3000 CA Rotterdam, the Netherlands; <sup>10</sup>Department of Obstetrics and Gynecology, Hôpital Universitaire Robert Debré, 75019 Paris, France; <sup>11</sup>Stem Cells and Regenerative Medicine, Birth Defects Research Centre, UCL Great Ormond Street Institute of Child Health, University College London, WC1N 1EH London, UK; <sup>12</sup>Department of Pediatric Surgery, Erasmus University Medical Center, 3000 CA Rotterdam, the Netherlands

<sup>13</sup>These authors contributed equally to this work

\*Correspondence: [r.hofstra@erasmusmc.nl](mailto:r.hofstra@erasmusmc.nl) (R.M.W.H.), [m.alves@erasmusmc.nl](mailto:m.alves@erasmusmc.nl) (M.M.A.)

<http://dx.doi.org/10.1016/j.ajhg.2017.05.011>

© 2017 American Society of Human Genetics.

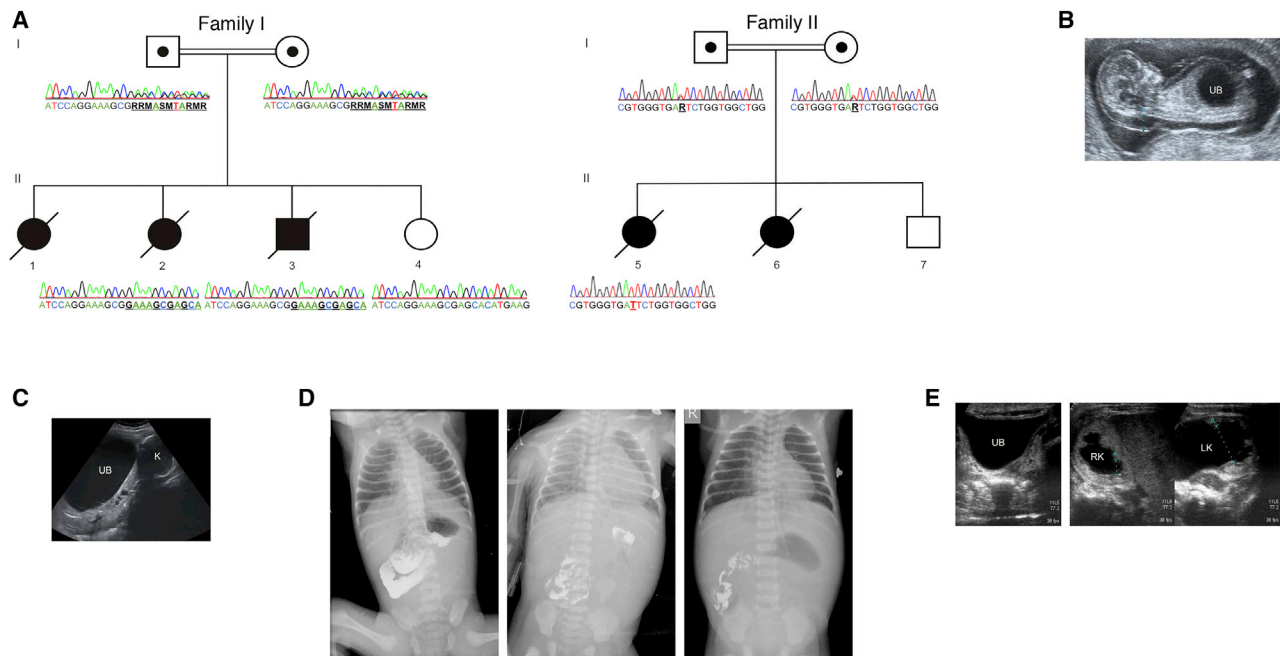


**Figure 1. Genetic Analysis and Description of the Three MMIHS Subjects Included in This Study**

(A) Pedigrees of the two consanguineous families analyzed by Sanger sequencing show the presence of homozygous variants in *MYLK*. Subject 1 (II-2) and subject 2 (II-3) carry a 7 bp duplication in exon 23 (c.3838\_3844dupGAAAGCG [p.Glu1282\_Glyfs\*51]), whereas their unaffected sister (II-4) shows no mutant allele. Subject 3 (II-5) has a putative splice-site variant affecting exon 23 (c.3985+5C>A). Both variants are present in a heterozygous state in the parents.

(B) Prenatal ultrasonography of subject 1 (II-2) at 13 weeks of gestation revealed a distended bladder and generalized subcutaneous edema.

(C) Prenatal ultrasonography of subject 2 (II-3) at 24 weeks revealed a distended bladder, hydronephrosis, and severe oligohydramnios.

(D) Barium enema performed in subject 2 (II-3) suggested intestinal obstruction and malrotation.

(E) Neonatal ultrasonography of subject 3 (II-5) revealed bladder distension and bilateral hydronephrosis.

Abbreviations are as follows: UB, urinary bladder; K, kidney; RK, right kidney; and LK, left kidney.

couple of Indian origin. The antenatal period was complicated with polyhydramnios, but the baby was born at term by normal delivery. No neonatal complications were reported. At 2 days of age, she was admitted back to the hospital with bilious vomiting. Barium enema confirmed intestinal obstruction, which was most likely caused by malrotation of the intestine (Figure 1D). Surgery was performed 1 day later to place an ileostomy and correct the intestinal malrotation. During surgery, a distal micro-colon was revealed, and the bladder was catheterized. Histopathological analysis of the mid-ileum identified the presence of ganglia. Abdominal ultrasound revealed distension of the bladder and bilateral hydronephrosis (Figure 1E), allowing the diagnosis of MMIHS to be made. Further follow-up of the family revealed that a younger sister (II-6 in Figure 1A) of subject 3 had also been diagnosed with MMIHS.

To identify the genetic cause of the disease in these subjects, we used a combined strategy of homozygosity mapping and whole-exome sequencing (WES). Written informed consent was obtained from the parents, and this study was approved by the Erasmus Medical Center ethics committee (Medisch Ethische Toetsings commissie 2011/148, Algemeen Beoordelings en Registratieformulier form NL35920.042.11) and by the institutional review

board at Baylor College of Medicine (Baylor Hopkins Centers for Mendelian Genomics protocol H-29697). Absence of heterozygosity (AOH), copy-number variants (CNVs), and exonic variants with deleterious changes predicted in silico (single-nucleotide variants [SNVs] and insertions or deletions) were determined as previously described.<sup>10</sup> Because consanguinity is known to increase the number of regions of shared haplotypes and is therefore associated with the occurrence of autosomal-recessive disorders,<sup>11,12</sup> we analyzed the filtered variants by identifying regions that are presumed to be shared identically by descent in extended genomic intervals of AOH. These identical-by-descent (IBD) regions are enriched with potential deleterious variants fulfilling Mendelian expectations<sup>13</sup> and were the starting point of our genetic analysis. For subject 1 (II-2 in Figure 1A), 55 homozygous regions of at least 1 Mb in length and harboring at least 50 probes were identified by SNP arrays. Of these 55 regions, 38 were present in the parents in a heterozygous state (Figure S1 and Table S1) and were likely to be IBD regions. Analysis of the SNP arrays did not identify any deleterious large CNVs. WES was also performed for subject 1, and the filtering criteria followed are described in Figure S2. Out of 2,848 rare variants found (minor allele frequency below 1%), only 20 were proven to be recessively inherited and predicted to

**Table 1. Prioritized Rare Recessive Variants Present in AOH Regions and Predicted to Be Deleterious in Subject 1**

Gene	Type	Exon	Effect	HGVS Genomic Change (GenBank ID)	cDNA	Protein	CADD Phred Score
<i>DENND4B</i>	Ins	18	F	g.153907306_153907307ins GCTGCTGC (NC_000001.10)	c.2702_2703ins GCAGCAGC	p.Gln904Hisfs*48	32
<i>LENEP</i>	SNV	1	MS	g.154966258C>G (NC_000001.10)	c.175C>G	p.Leu59Val	23.6
<i>SPTA1</i>	SNV	14	SP	g.158639351C>G (NC_000001.10)	c.1680G>C	–	23.1
<i>ITLN1</i>	SNV	8	MS	g.160846459G>A (NC_000001.10)	c.937C>T	p.Arg313Cys	24
<i>MCM6</i>	SNV	17	MS	g.136598443A>G (NC_000002.11)	c.2428T>C	p.Tyr810His	24.2
<i>MYLK</i>	Ins	23	F	g.123383093_123383099dup (NC_000003.11)	c.3838_3844dup GAAAGCG	p.Glu1282Glyfs*51	36
<i>AFF1</i>	SNV	5	SP	g.88011230C>T (NC_000004.11)	c.1170+8C>T	–	4.535
<i>ADAMTS16</i>	SNV	16	MS	g.5239937C>T (NC_000005.9)	c.2422C>T	p.Arg808Trp	25.7
<i>ID4</i>	SNV	1	MS	g.19838067C>G (NC_000006.11)	c.82C>G	p.Leu28Val	25.7
<i>ZNF596</i>	Del	4	CSP	g.193799_193812delCTGCAAG GTGAGCT (NC_000008.10)	c.217_223+7delCT GCAAGGTGAGCT	–	23.2
<i>C8orf34</i>	SNV	13	S, SP	g.69728122T>C (NC_000008.10)	c.1551T>C	–	6.825
<i>PKHD1L1</i>	SNV	71	MS	g.110523018A>G (NC_000008.10)	c.11408A>G	p.His3803Arg	24.2
<i>TRPM6</i>	SNV	18	MS	g.77411729C>G (NC_000009.11)	c.2319G>C	p.Gln773His	26.1
<i>CCDC81</i>	SNV	4	MS	g.86103688C>T (NC_000011.9)	c.404C>T	p.Ser135Leu	28.3
<i>METTL7B</i>	SNV	1	MS	g.56075840C>T (NC_000012.11)	c.302C>T	p.Pro101Leu	33
<i>EXD1</i>	SNV	8	MS	g.41488231G>C (NC_000015.9)	c.539C>G	p.Ala180Gly	24.5
<i>DUOX2</i>	SNV	30	SP	g.45388019C>T (NC_000015.9)	c.4080+7G>A	–	5.471
<i>AARS</i>	SNV	6	MS	g.70304215G>A (NC_000016.9)	c.700C>T	p.Pro234Ser	28.9
<i>NSF</i>	SNV	20	MS	g.44832731G>A (NC_000017.10)	c.2209G>A	p.Gly737Arg	33
<i>USP29</i>	SNV	4	MS	g.57642673G>A (NC_000019.9)	c.2630G>A	p.Gly877Glu	24.4

Abbreviations are as follows: AOH, absence of heterozygosity; Ins, insertion; Del, deletion; SNV, single-nucleotide variant; MS, missense variant; F, frameshift variant; S, synonymous variant; SP, putative splice variant; ncRNA, non-coding RNA; and CSP, canonical splice site.

be deleterious (Table 1). From this list, one gene stood out because of its known biological function in the contraction of SMC: myosin light chain kinase (*MYLK* [OMIM: 600922]). In this gene, subject 1 carried an exon 23 duplication that led to a frameshift and to the appearance of an early stop codon at the beginning of exon 24 (c.3838\_3844dupGAAAGCG [p.Glu1282Glyfs\*51] [GenBank: NM\_053025.3]). It is unlikely that this duplication resulted from secondary structure mutagenesis given that the surrounding sequence is not palindromic. *MYLK* was also located in an AOH region of 3 Mb (Table S1). Previous studies have shown that mice lacking the smooth muscle *Mylk* isoform have severe gut dysmotility and abnormal function of the bladder,<sup>14</sup> a phenotype reminiscent of that described for individuals affected by MMIHS. Moreover, according to data from the Human Integrated Protein Expression Database and the Genotype-Tissue Expression project<sup>15</sup> in GeneCards,<sup>16</sup> *MYLK* was the only gene in this list with expression in human fetal gut and bladder, the two major organs affected in MMIHS. On the basis of this evidence, we considered *MYLK* to be the best candidate gene for this family.

WES investigations of another independent cohort of individuals consisting of 42 probands with visceral myopathy, MMIHS, and prune-belly phenotypes<sup>5</sup> led to the identification of one subject, subject 3 (II-5 in Figure 1A), in whom a homozygous putative splice variant affecting exon 23 of *MYLK* (c.3985+5C>A [GenBank: NM\_053025.3]) had also been identified. Analysis of the AOH regions present in this subject showed that stretches of homozygosity composed 8% of her genome and that *MYLK* was located within a 9 Mb genomic region of AOH (Figure S3 and Table S2). It is also worth noting that combined analysis of the WES data generated for subject 1 (Table 1) and subject 3 (Table 2) showed that *MYLK* was the only shared gene in which recessive variants predicted to be deleterious had been identified (Figure S2). Sanger sequencing performed with specific primers (*MYLKF* and *MYLKR*; Table S3) confirmed the presence of both variants in a homozygous state in these subjects and showed that they were inherited from heterozygous parents (Figure 1A). Subject 2 (II-3 in Figure 1A) was also found to carry the same homozygous duplication detected in subject 1 (II-2 in Figure 1A), whereas their unaffected sister

**Table 2. Prioritized Rare Recessive Variants Present in Subject 3**

Gene	Type	Exon	Effect	HGVS Genomic Change (GenBank ID)	cDNA	Protein	CADD Phred Score
<i>THUMPD2</i>	SNV	3	MS	g.399966996C>A (NC_000002.11)	c.526G>T	p.Asp176Tyr	25.4
<i>NBEAL2</i>	SNV	32	MS	g.47043984C>T (NC_000003.11)	c.5275C>T	p.Arg1759Cys	26.8
<i>RNF123</i>	SNV	24	MS	g.49743006G>A (NC_000003.11)	c.2198G>A	p.Arg733Gln	24.4
<i>IFRD2</i>	SNV	2	MS	g.50328075T>C (NC_000003.11)	c.286A>G	p.Ser96Gly	25.4
<i>CACNA2D3</i>	SNV	9	MS	g.54615858C>G (NC_000003.11)	c.917C>G	p.Pro306Arg	31
<i>IL17RD</i>	SNV	10	MS	g.57136593A>G (NC_000003.11)	c.893T>C	p.Ile298Thr	28.4
<i>MYLK</i>	SNV	23	SP	g.123382947C>A (NC_000003.11)	c.3985+5G>T	–	21.4
<i>SEC24D</i>	SNV	2	SP	g.119754899C>T (NC_000004.11)	c. –41–7G>A	–	9.701
<i>SLC26A5</i>	SNV	16	MS	g.103019758T>C (NC_000007.13)	c.1609A>G	p.Ile537Val	23.6
<i>CNTLN</i>	SNV	22	SP	g.17465974T>C (NC_000009.11)	c.3532–5T>C	–	12.13
<i>EHMT1</i>	SNV	12	S	g.140671136C>A (NC_000009.11)	c.1858C>A	–	20.8
<i>SIGLEC1</i>	Del	21	F	g.3669236delT (NC_000020.10)	c.5101delA	p.Thr1701Profs*26	33

Abbreviations are as follows: SNV, single-nucleotide variant; MS, missense variant; F, frameshift variant; S, synonymous variant; and SP, putative splice variant.

showed no mutant allele (Figure 1A). No genetic information was available for the older sister of subjects 1 and 2 or for the younger sister and brother of subject 3 as a result of DNA unavailability.

In humans, three major *MYLK* isoforms exist: a long isoform referred to as non-muscle *MYLK*, a short isoform known as smooth muscle *MYLK*, and a very small isoform called telokin.<sup>17</sup> The variants identified in the families included in this study affect both the long and the short isoforms (Figure S4). To further evaluate the involvement of *MYLK* in MMIHS pathogenesis, we determined the presence of this protein at different stages of human embryonic development. Because the bladder and intestine are the two organs affected in MMIHS, we used a specific antibody to evaluate the presence of *MYLK* in these organs by immunohistochemistry. Formalin-fixed paraffin-embedded human small intestinal and bladder specimens obtained from control samples were retrieved from the Biobank of the Pathology Department of the Erasmus University Medical Center. We observed that, across all developmental stages included in this study, *MYLK* was localized in all SMCs that form all muscular layers of the intestine and bladder (Figure 2A). We also immunostained specimens collected from the small intestine and bladder of subject 1 (II-2 in Figure 1A) by the Department of Pathology of the Hôpital Universitaire Robert Debré and found no signal for *MYLK*. Because the recognition epitope of the antibody used is located before the homozygous duplication (amino acids 908–938), it is likely that *MYLK* expression is abolished in this subject, confirming loss of function and pathogenicity of the variant identified (Figure 2B). Surprisingly, no changes in the levels of neurofilament, c-Kit/CD117, tryptase, or ACTA2 were detected in this subject. Moreover, in comparison with age-matched control samples, the structure and cellular constituents of

the bladder and intestine showed no apparent pathological abnormalities (Figure 2C). This suggests that although *MYLK* is instrumental for the proper function of SMCs, its presence is not required for maintaining the structural architecture of these organs.

We also investigated the pathogenicity of the putative splice-site variant (c.3985+5C>A) found in subject 3 (II-5 in Figure 1A) by performing splicing assays as previously described.<sup>18</sup> Wild-type (WT) and mutant constructs were generated with genomic DNA from control and affected subjects with a primer set designed to include the genomic sequence that stretches from the last part of intron 22 of *MYLK* to the beginning of intron 23 (MinigeneF and MinigeneR; Table S3). Whereas the WT construct generated a transcript with the expected size (414 bp), the mutant construct eliminated all transcription products seen in the WT situation and produced a band with the same size as the empty vector. This result indicates that the identified variant is indeed a splice variant likely leading to the skipping of exon 23 (Figure 2D). As a consequence, a frameshift will occur and lead to the appearance of an early stop codon at the beginning of exon 24, but in a different location than the one identified in subjects 1 and 2. Although tissue specimens were not available for subject 3 (II-5 in Figure 1A), we suspect that expression of *MYLK* is also impaired, given that the splice variant had an effect similar to that of the duplication described for subjects 1 and 2 and is therefore likely to result in loss of function. Interestingly, we noticed that several other transcripts were generated for exon 23 in the WT situation, suggesting that this exon might normally be targeted for alternative splicing.

*MYLK* encodes an important kinase required for phosphorylation of the regulatory light chain (RLC) of myosin, leading to its activation and subsequent interaction with



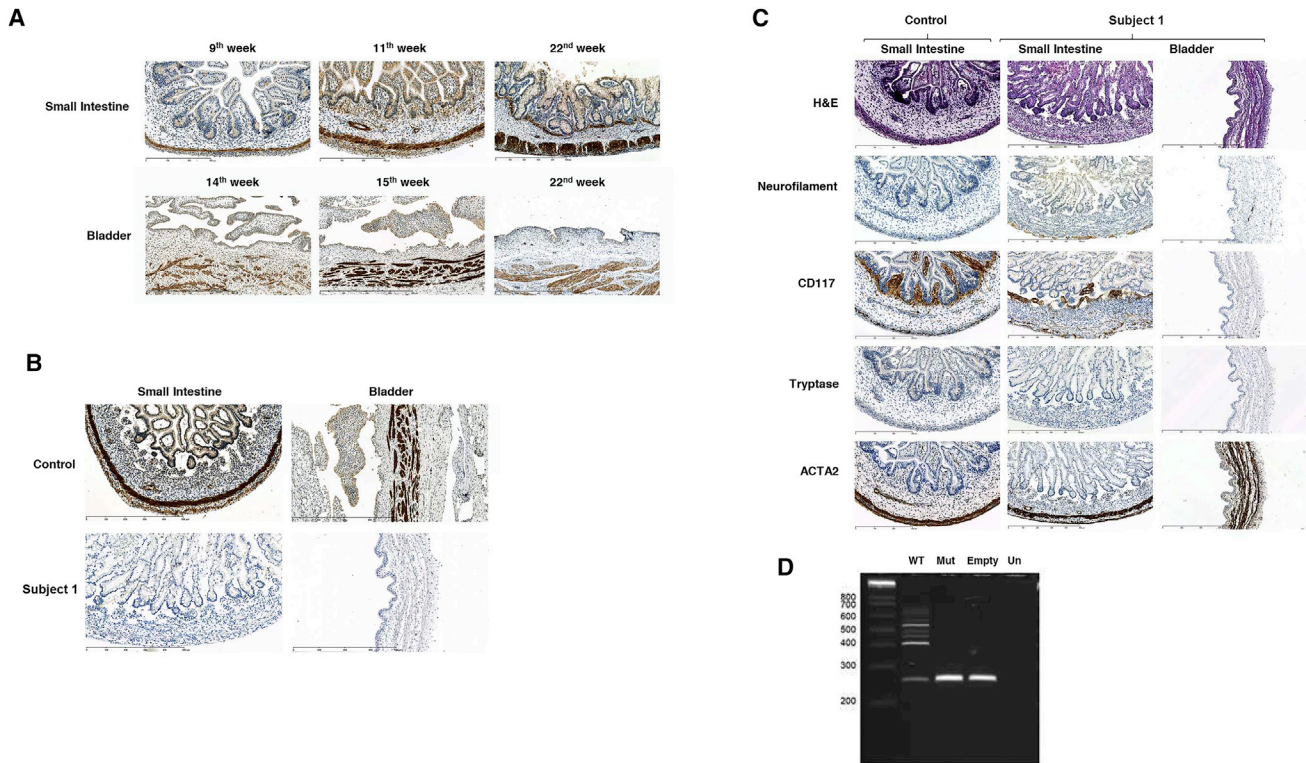


**Figure 2. Evaluation of the Effect of the *MYLK* Variants Identified**

(A) Immunohistochemistry performed in control specimens with a specific *MYLK* antibody (1:100; Thermo Fisher Scientific) showed that *MYLK* is present in SMCs that constitute muscular structures of the intestine and the bladder, including muscularis mucosa, blood vessels, and circular and longitudinal muscles of the muscularis propria. Similar patterns and expression levels were present throughout all developmental stages included in this study.

(B) *MYLK* is absent in the intestine and bladder of subject 1 (II-2 in Figure 1A).

(C) H&E staining and immunostainings performed in specimens derived from control samples and subject 1 with specific antibodies against neurofilament (1:600; Monosan), c-Kit/CD117 (1:200; Cell Marque), tryptase (1:1,600; Dako), and ACTA2 (ready to use; Dako) showed no significant differences.

(D) Splicing assays revealed impaired splicing of exon 23 of *MYLK* in subject 3 (II-5 in Figure 1A). SD6 and SA2 primers (Table S3) were used for evaluating transcripts produced by the wild-type (WT) vector, the mutant (Mut) vector containing the putative splice-site variant c.3985+5C>A, the empty vector (Empty), and untransfected cells (Un) according to a standard PCR protocol.

actin filaments<sup>17</sup> (Figure S5). This interaction is essential for SMC contraction, a mechanism that is already known to be defective in MMIHS.<sup>4,7,10</sup> According to our results, *MYLK* expression is most likely impaired in the subjects included in this study, and we expect that myosin activation cannot occur because of a lack of phosphorylation of its RLC. As a consequence, myosin will be unable to interact with actin, resulting in impaired SMC contractility (Figure S5). Considering that *MYLK* is a ubiquitous protein, it is surprising that the phenotype seen in individuals affected with MMIHS, as well as in the conditional-knockout mouse,<sup>14</sup> is restricted to the intestine and bladder. This might be related to the fact that the extra visceral phenotypes develop only later in life, and we were unable to detect it because none of our subjects survived longer than a few days after birth. This hypothesis is supported by previous reports linking heterozygous loss of *MYLK* to aortic vascular smooth muscle defects.<sup>19,20</sup> In these subjects, aneurysms often occur without preceding dilatation of the aorta, suggesting that it takes time for the reduction of *MYLK* to take its toll on major

blood vessels. However, it could also be that other kinases are able to salvage SMC contraction of the extra-visceral organs. This hypothesis is supported by the fact that RLC phosphorylation could still be induced in aortic cells collected from mice where expression of all three *Mylk* isoforms is abolished.<sup>21</sup> Considering that the heterozygous parents of the subjects included in this study do not show any cardiac problems as far as we know, the second hypothesis is perhaps more likely, but further studies need to be performed to bring new insight into this matter.

In conclusion, we provide evidence for *MYLK* involvement in MMIHS, confirming that this is a heterogeneous disease of the visceral organs where disruption of SMC contraction seems to be the major trigger for pathogenicity.

#### Accession Numbers

The accession numbers for variants c.3838\_3844dupGAAAGCG and c.3985+5C>A are ClinVar: SCV000299345 and SCV000574720, respectively.

## Supplemental Data

Supplemental Data include five figures and three tables and can be found with this article online at <http://dx.doi.org/10.1016/j.ajhg.2017.05.011>.

## Conflicts of Interest

The Department of Molecular and Human Genetics at the Baylor College of Medicine derives revenue from molecular testing offered at Baylor Genetics Laboratories. J.R.L. has stock ownership in 23andMe, is a paid consultant for Regeneron Pharmaceuticals, has stock options in Lasergen Inc., is a member of the scientific advisory board of Baylor Genetics, and is a co-inventor on multiple United States and European patents related to molecular diagnostics for inherited neuropathies, eye diseases, and bacterial genomic fingerprinting.

## Acknowledgments

The authors would like to thank the two families described in this manuscript for their cooperation and willingness to be part of this study. The authors would also like to thank Dr. Raj Kapur for his help with the analysis of the immunohistochemistry data and Tom de Vries Lentsch for making Figure S5. This work received funding from the National Human Genome Research Institute and the National Heart, Lung, and Blood Institute (UM1 HG006542) to the Baylor-Hopkins Center for Mendelian Genomics and from the Stitching Sophia Kinderziekenhuis Fonds (S15-30) to R.M.W.H. and M.M.A.

Received: April 10, 2017

Accepted: May 11, 2017

Published: June 8, 2017

## Web Resources

ClinVar, <http://www.ncbi.nlm.nih.gov/clinvar/>

OMIM, <https://www.omim.org/>

GenBank, <https://www.ncbi.nlm.nih.gov/genbank/>

## References

1. Kamm, K.E., and Stull, J.T. (2001). Dedicated myosin light chain kinases with diverse cellular functions. *J. Biol. Chem.* *276*, 4527–4530.
2. Berdon, W.E., Baker, D.H., Blanc, W.A., Gay, B., Santulli, T.V., and Donovan, C. (1976). Megacystis-microcolon-intestinal hypoperistalsis syndrome: a new cause of intestinal obstruction in the newborn. Report of radiologic findings in five newborn girls. *AJR Am. J. Roentgenol.* *126*, 957–964.
3. Wymer, K.M., Anderson, B.B., Wilkens, A.A., and Gundeti, M.S. (2016). Megacystis microcolon intestinal hypoperistalsis syndrome: Case series and updated review of the literature with an emphasis on urologic management. *J. Pediatr. Surg.* *51*, 1565–1573.
4. Thorson, W., Diaz-Horta, O., Foster, J., 2nd, Spiliopoulos, M., Quintero, R., Farooq, A., Blanton, S., and Tekin, M. (2014). De novo ACTG2 mutations cause congenital distended bladder, microcolon, and intestinal hypoperistalsis. *Hum. Genet.* *133*, 737–742.
5. Wangler, M.F., Gonzaga-Jauregui, C., Gambin, T., Penney, S., Moss, T., Chopra, A., Probst, F.J., Xia, F., Yang, Y., Werlin, S., et al.; Baylor-Hopkins Center for Mendelian Genomics (2014). Heterozygous *de novo* and inherited mutations in the smooth muscle actin (*ACTG2*) gene underlie megacystis-microcolon-intestinal hypoperistalsis syndrome. *PLoS Genet.* *10*, e1004258.
6. Tuzovic, L., Tang, S., Miller, R.S., Rohena, L., Shahmirzadi, L., Gonzalez, K., Li, X., LeDuc, C.A., Guo, J., Wilson, A., et al. (2015). New Insights into the Genetics of Fetal Megacystis: *ACTG2* Mutations, Encoding  $\gamma$ -2 Smooth Muscle Actin in Megacystis Microcolon Intestinal Hypoperistalsis Syndrome (Berdon Syndrome). *Fetal Diagn. Ther.* *38*, 296–306.
7. Halim, D., Hofstra, R.M., Signorile, L., Verdijk, R.M., van der Werf, C.S., Sribudiani, Y., Brouwer, R.W., van IJcken, W.F., Dahl, N., Verheij, J.B., et al. (2016). *ACTG2* variants impair actin polymerization in sporadic Megacystis Microcolon Intestinal Hypoperistalsis Syndrome. *Hum. Mol. Genet.* *25*, 571–583.
8. Matera, I., Rusmini, M., Guo, Y., Lerone, M., Li, J., Zhang, J., Di Duca, M., Nozza, P., Mosconi, M., Pini Prato, A., et al. (2016). Variants of the *ACTG2* gene correlate with degree of severity and presence of megacystis in chronic intestinal pseudo-obstruction. *Eur. J. Hum. Genet.* *24*, 1211–1215.
9. Gauthier, J., Ouled Amar Bencheikh, B., Hamdan, F.F., Harrison, S.M., Baker, L.A., Couture, F., Thiffault, I., Ouazzani, R., Samuels, M.E., Mitchell, G.A., et al. (2015). A homozygous loss-of-function variant in *MYH11* in a case with megacystis-microcolon-intestinal hypoperistalsis syndrome. *Eur. J. Hum. Genet.* *23*, 1266–1268.
10. Halim, D., Wilson, M.P., Oliver, D., Brosens, E., Verheij, J.B.G.M., Han, Y., Nanda, V., Lyu, Q., Doukas, M., Stoop, H., et al. (2017). Loss of *LMOD1* impairs smooth muscle contractility and causes megacystis microcolon intestinal hypoperistalsis syndrome in humans and mice. *Proc. Natl. Acad. Sci. USA* *114*, E2739–E2747.
11. Hamamy, H., Antonarakis, S.E., Cavalli-Sforza, L.L., Temtamy, S., Romeo, G., Kate, L.P., Bennett, R.L., Shaw, A., Megarbane, A., van Duijn, C., et al. (2011). Consanguineous marriages, pearls and perils: Geneva International Consanguinity Workshop Report. *Genet. Med.* *13*, 841–847.
12. Hamamy, H. (2012). Consanguineous marriages: Preconception consultation in primary health care settings. *J. Community Genet.* *3*, 185–192.
13. Szpiech, Z.A., Xu, J., Pemberton, T.J., Peng, W., Zöllner, S., Rosenberg, N.A., and Li, J.Z. (2013). Long runs of homozygosity are enriched for deleterious variation. *Am. J. Hum. Genet.* *93*, 90–102.
14. He, W.Q., Peng, Y.J., Zhang, W.C., Lv, N., Tang, J., Chen, C., Zhang, C.H., Gao, S., Chen, H.Q., Zhi, G., et al. (2008). Myosin light chain kinase is central to smooth muscle contraction and required for gastrointestinal motility in mice. *Gastroenterology* *135*, 610–620.
15. GTEx Consortium (2013). The Genotype-Tissue Expression (GTEx) project. *Nat. Genet.* *45*, 580–585.
16. Fishilevich, S., Zimmerman, S., Kohn, A., Iny Stein, T., Olander, T., Kolker, E., Safran, M., and Lancet, D. (2016). Genic insights from integrated human proteomics in GeneCards. *Database (Oxford)* *2016*, baw030.
17. Hong, F., Haldeman, B.D., Jackson, D., Carter, M., Baker, J.E., and Cremo, C.R. (2011). Biochemistry of smooth muscle

- myosin light chain kinase. *Arch. Biochem. Biophys.* 510, 135–146.
18. Van Der Werf, C.S., Wabbersen, T.D., Hsiao, N.H., Paredes, J., Etchevers, H.C., Kroisel, P.M., Tibboel, D., Babarit, C., Schreiber, R.A., Hoffenberg, E.J., et al. (2012). *CLMP* is required for intestinal development, and loss-of-function mutations cause congenital short-bowel syndrome. *Gastroenterology* 142, 453–462.e3.
  19. Wang, L., Guo, D.C., Cao, J., Gong, L., Kamm, K.E., Regalado, E., Li, L., Shete, S., He, W.Q., Zhu, M.S., et al. (2010). Mutations in myosin light chain kinase cause familial aortic dissections. *Am. J. Hum. Genet.* 87, 701–707.
  20. Hannuksela, M., Stattin, E.L., Klar, J., Ameer, A., Johansson, B., Sörensen, K., and Carlberg, B. (2016). A novel variant in *MYLK* causes thoracic aortic dissections: genotypic and phenotypic description. *BMC Med. Genet.* 17, 61.
  21. Somlyo, A.V., Wang, H., Choudhury, N., Khromov, A.S., Majesky, M., Owens, G.K., and Somlyo, A.P. (2004). Myosin light chain kinase knockout. *J. Muscle Res. Cell Motil.* 25, 241–242.

**Supplemental Data**

**Loss-of-Function Variants in *MYLK***

**Cause Recessive Megacystis Microcolon**

**Intestinal Hypoperistalsis Syndrome**

**Danny Halim, Erwin Brosens, Françoise Muller, Michael F. Wangler, Arthur L. Beaudet, James R. Lupski, Zeynep H. Coban Akdemir, Michael Doukas, Hans J. Stoop, Bianca M. de Graaf, Rutger W.W. Brouwer, Wilfred F.J. van Ijcken, Jean-François Oury, Jonathan Rosenblatt, Alan J. Burns, Dick Tibboel, Robert M.W. Hofstra, and Maria M. Alves**



Figure S1: AOH regions present in subject 1



**Figure S2: Filtering criteria used to analyze the whole exome sequencing data of subject 1 and subject 3.** High quality variants with a read depth  $\geq 5$  were retained for further analysis. An allele frequency cut-off of 1% in public databases (ExAC release 0.3, ESP6500SI-V2; 1000 Genomes Phase 3 release v5.20130502 and GoNL SNPs and Indels release 5) was considered for homozygous variants. Only variants predicted to affect splicing, nonsense variants, and coding and non-coding variants with a CADD score above 20 (CADD v1.3) were prioritized as likely deleterious. Subject 1 and subject 3 shared two genes with autosomal recessive variants. However, only *MYLK* had variants predicted to be deleterious and was expressed in fetal gut and bladder, the two major organs affected in MMIHS.

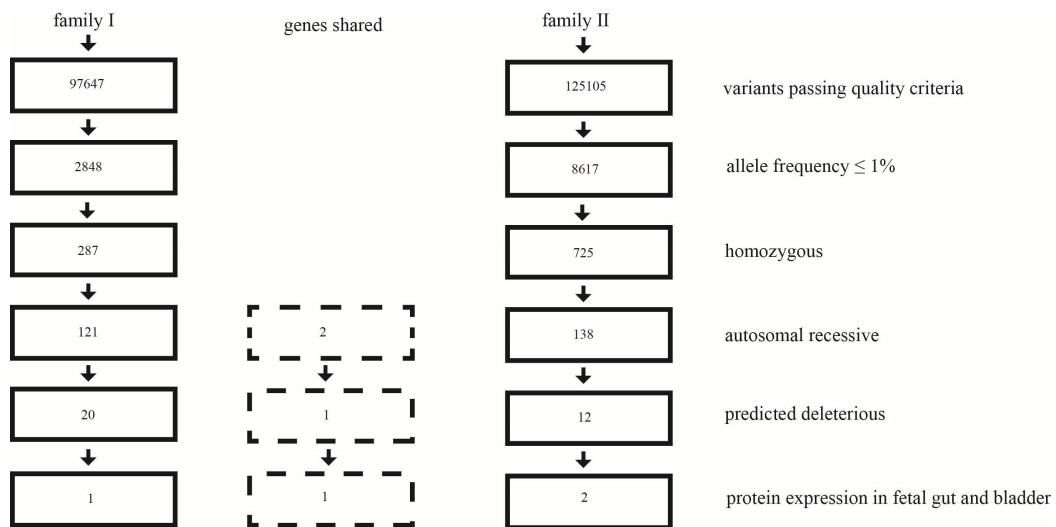
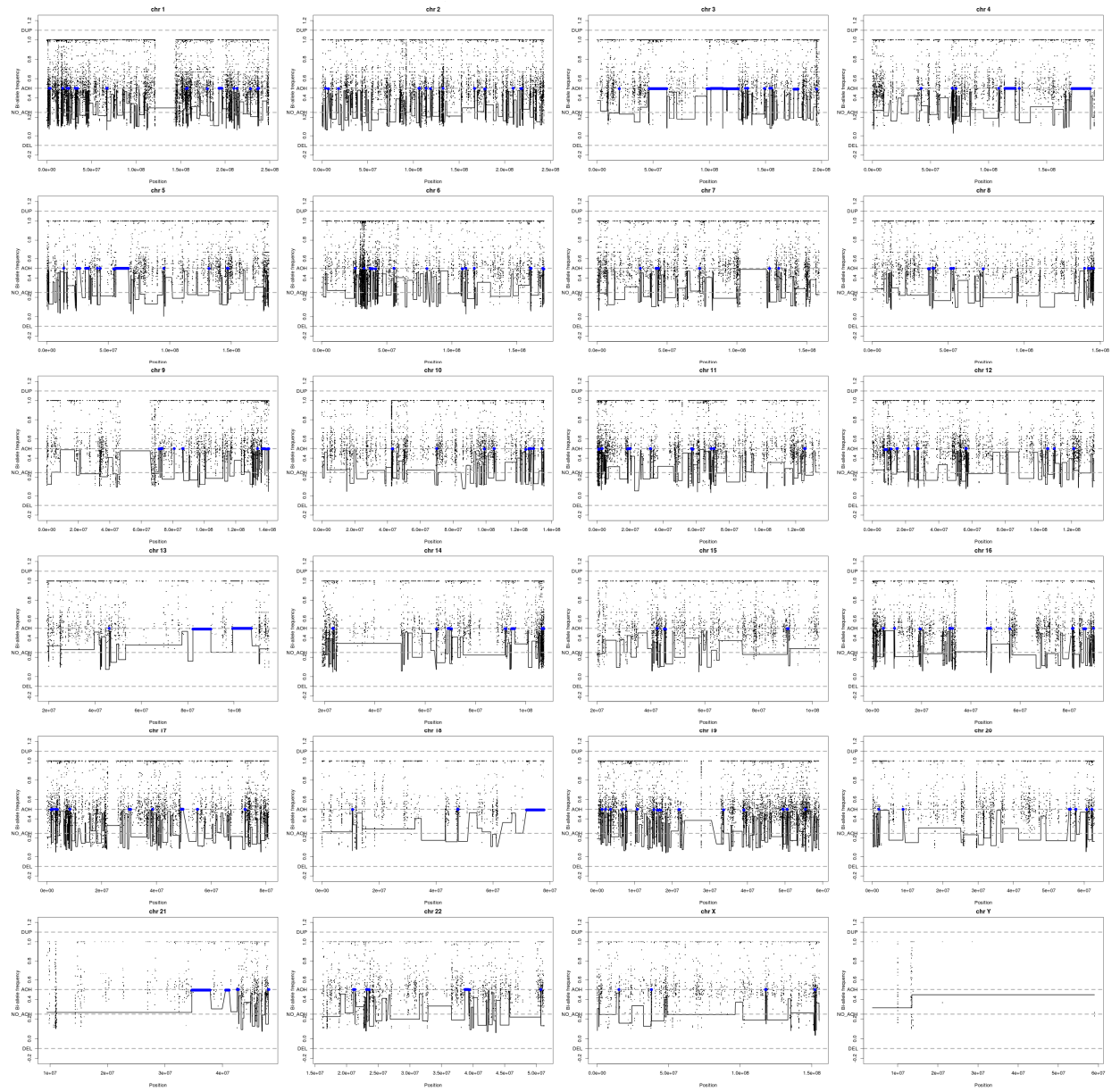
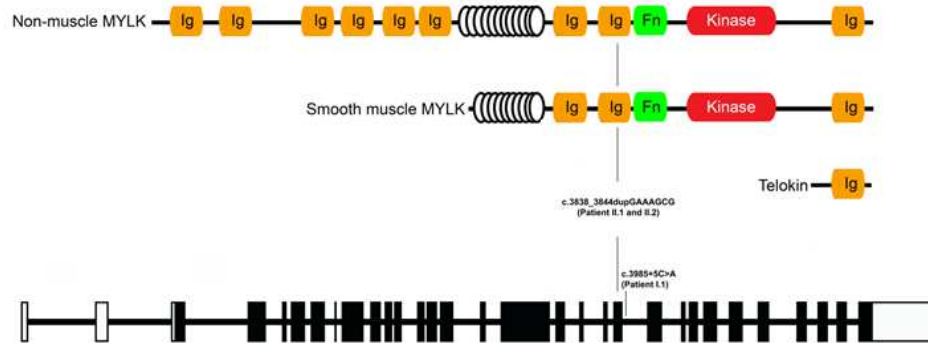


Figure S3: AOH regions present in subject 3



**Figure S4: Schematic representation of *MYLK* with its 33 exons and its three *major* isoforms, with the variants identified in MMIHS affected individuals depicted.**



**Figure S5: Schematic illustration of the molecular mechanisms required for SMC contraction and the effect of impaired *MYLK* expression on this mechanism.** In the wild type situation, MYLK phosphorylates the regulatory light chain (RLC) of myosin, leading to its activation and subsequent interaction with actin filaments. As a consequence, SMCs contraction occurs. In the presence of any of the variants identified, *MYLK* expression is impaired, and phosphorylation of the RLC cannot occur. Therefore, myosin is unable to interact with actin filaments and SMC contraction is impaired.

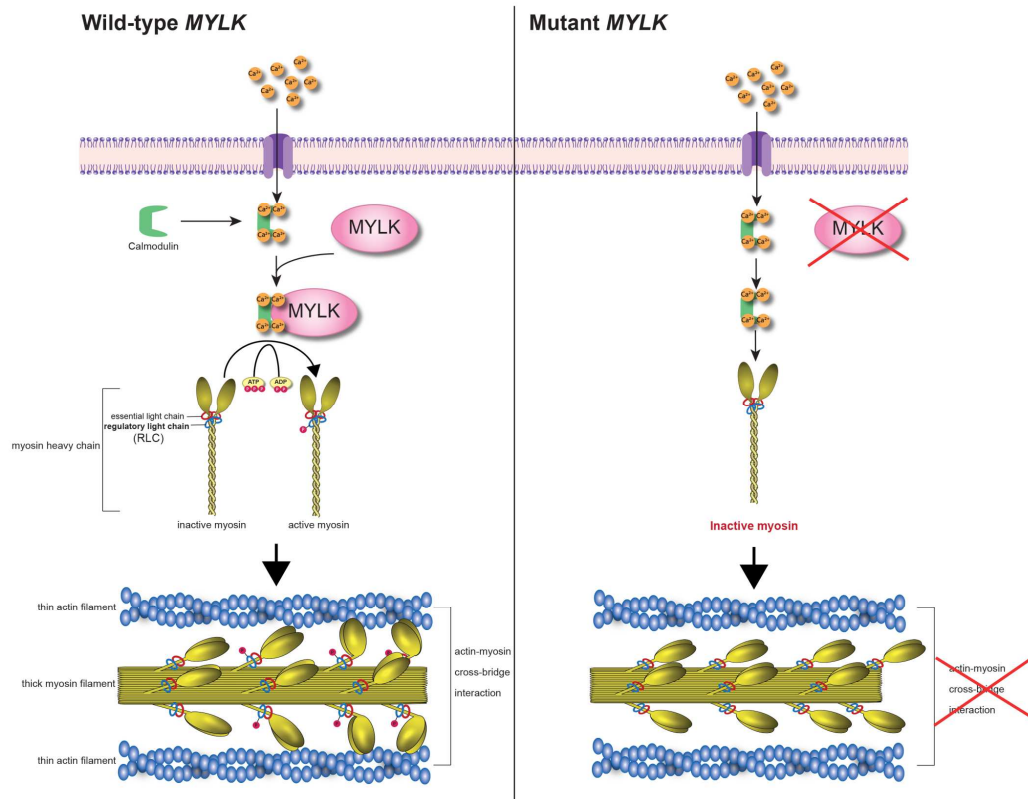




**Table S1: ROH regions present in subject 1 (>1MB)**

Chr.	ROH region	Size (kb)
1	chr1:242944438-244084838	1140400
1	chr1:145416055-147826789	2410734
1	chr1:150856155-165465569	14609414
1	chr1:70267535-120553638	50286103
2	chr2:193957725-194971610	1013885
2	chr2:228026937-231049859	3022922
2	chr2:132604119-139882966	7278847
2	chr2:231059532-240330999	9271467
3	chr3:120385537-121923035	1537498
3	chr3:121931699-124830052	2898353
4	chr4:87160439-91509561	4349122
4	chr4:77709496-86985942	9276446
5	chr5:92602370-93717798	1115428
5	chr5:41416674-42624527	1207853
5	chr5:87090359-88357858	1267499
5	chr5:179620442-180915260	1294818
5	chr5:1483897-8953381	7469484
6	chr6:15067080-19041846	3974766
6	chr6:19050234-25173355	6123121
7	chr7:122810117-123980215	1170098
7	chr7:101954468-103191686	1237218
7	chr7:40483744-43163338	2679594
7	chr7:29178667-40443341	11264674
8	chr8:0-2683108	2683108
8	chr8:46886735-119798778	72912043
9	chr9:70984372-84389822	13405450
11	chr11:54794237-56482051	1687814
11	chr11:79726393-91682741	11956348
12	chr12:42347636-71689131	29341495
13	chr13:23646794-24668110	1021316
15	chr15:36662007-54162140	17500133
16	chr16:68580385-73593216	5012831
17	chr17:44287381-45879796	1592415
17	chr17:41687610-44278785	2591175
18	chr18:334419-3513265	3178846
19	chr19:55569398-59128983	3559585
20	chr20:0-1613328	1613328
22	chr22:18922645-21800198	2877553

**Table S2: ROH regions present in subject 3 (>1MB)**

<b>Chr.</b>	<b>ROH region</b>	<b>Size (kb)</b>
1	Chr1:192999051-196461513	3462462
2	Chr2:23785517-24914125	1128608
2	Chr2:38809162-42181226	3372064
2	Chr2:47748292-48935849	1187557
2	Chr2:214228792-216256775	2027983
2	Chr2:217541582-218713924	1172342
3	Chr3:46480801-62229553	15748752
3	Chr3:97982936-101389864	3406928
3	Chr3:101443461-111936564	10493103
3	Chr3:111958510-115528917	3570407
3	Chr3:116163902-126070625	9906723
3	Chr3:175345143-178978718	3633575
4	Chr4:114028149-122683007	8654858
4	Chr4:171525788-187530313	16004525
5	Chr5:24510242-26915466	2405224
5	Chr5:31532429-34124590	2592161
5	Chr5:56271822-66480004	10208182
5	Chr5:112101793-114462589	2360796
5	Chr5:159776047-161128914	1352867
6	Chr6:37897839-39162227	1264388
6	Chr6:91278482-97096363	5817881
7	Chr7:64721546-66262309	1540763
7	Chr7:102330349-121081115	18750766
8	Chr8:136560952-139190957	2630005
9	Chr9:8518143-17579198	9061055
9	Chr9:46386688-65636192	19249504
9	Chr9:114985985-116130371	1144386
9	Chr9:136944465-138646881	1702416
9	Chr9:138656707-139944509	1287802
10	Chr10:19498278-20568524	1070246
10	Chr10:92813181-93841227	1028046
11	Chr11:18956194-20127046	1170852
11	Chr11:62064841-64525464	2460623
11	Chr11:65623347-67572698	1949351
12	Chr12:7463491-8688999	1225508
13	Chr13:82265231-90015578	7750347
13	Chr13:99449898-107516570	8066672
14	Chr14:94391699-95556747	1165048
16	Chr16:5257260-8740015	3482755
16	Chr16:46637746-48118036	1480290
17	Chr17:4997039-6014176	1017137
18	Chr18:71740503-77927028	6186525
19	Chr19:8151418-10229521	2078103
20	Chr20:2277020-4704957	2427937
20	Chr20:35263266-36375071	1111805
21	Chr21:34668747-37834258	3165511

**Table S3: Primer sets used in this study**

<b>Primer</b>	<b>Sequence</b>
<i>MYLKF</i>	TCAGGGAAGCTGGACTCTGG
<i>MYLKR</i>	CAGGGAGTCTGTGGGTTGC
MinigeneF	GCCCCCTTCCTTTCCTAGCC
MinigeneR	GCAGGGAGTCTGTGGGTTGC
SD6F	TCTGAGTCACCTGGACAACC
SA2R	GCTCACAAATACCACTGAGAT